

## Seismic fragility curves for greek bridges: methodology and case studies

Ioannis F. Moschonas · Andreas J. Kappos ·  
Panagiotis Panetsos · Vissarion Papadopoulos ·  
Triantafyllos Makarios · Pavlos Thanopoulos

Received: 10 January 2008 / Accepted: 6 July 2008 / Published online: 10 September 2008  
© Springer Science+Business Media B.V. 2008

**Abstract** This study focusses on the estimation of seismic fragility curves for all common bridge types found in modern greek motorways. At first a classification scheme is developed in order to classify the existing bridges into a sufficient number of classes. A total of 11 representative bridge classes resulted, based on the type of piers, deck, and pier-to-deck connection. Then an analytical methodology for deriving fragility curves is proposed and applied to the representative bridge models. This procedure is based on pushover analysis of the entire bridge and definition of damage states in terms of parameters of the bridge pushover curves. The procedure differentiates the way of defining damage according to the seismic energy dissipation mechanism in each bridge, i.e. bridges with yielding piers of the column type and bridges with bearings (with or without seismic links) and non-yielding piers of the wall type. The activation of the abutment-backfill system due to closure of the gap between the deck and the abutments is also taken into account. The derived fragility curves are subjected to a first calibration against empirical curves based on damage data from the US and Japan.

---

I. F. Moschonas (✉) · A. J. Kappos  
Department of Civil Engineering, Aristotle University of Thessaloniki, Thessaloniki, Greece  
e-mail: jfmoschon@kat.forthnet.gr

A. J. Kappos  
e-mail: ajkap@civil.auth.gr

P. Panetsos  
EGNATIA ODOS SA, Thessaloniki, Greece  
e-mail: PPANE@egnatia.gr

V. Papadopoulos  
School of Civil Engineering, National Technical University, Athens, Greece  
e-mail: vpapado@central.ntua.gr

T. Makarios  
ITSAK, Institute of Engineering Seismology and Earthquake Engineering, Thessaloniki, Greece  
e-mail: makarios@itsak.gr

P. Thanopoulos  
DOMI SA, Athens, Greece  
e-mail: domi\_oe@hol.gr

**Keywords** Bridges · Vulnerability assessment · Fragility curves · Bridge classification · Pushover analysis · Damage states

## 1 Introduction

It is now common practice in assessing the seismic vulnerability of a large number of bridges to develop for each representative bridge class a set of fragility curves, each curve in the set corresponding to a specific damage state. The first step in this procedure is the classification of bridges into typological classes on the basis of selected parameters that affect their seismic response. The definition of an appropriate classification scheme is a significant step in the vulnerability assessment procedure. If the scheme is a very crude one, involving only few classes, it is only natural that some significant parameters affecting the vulnerability of bridges will be missed; it will then be impossible to use the results of fragility analysis to prioritize the bridge stock with a view to retrofitting, in a feasible way (i.e. by identifying a relatively limited number of bridges that are appropriate candidates for retrofit). In the other extreme case of a very detailed classification scheme, the fragility assessment procedure becomes time-consuming and strenuous, if at all feasible. Furthermore, the calibration of the resulting curves is impossible for most of the bridge classes due to lack of actual seismic bridge damage data for these classes (Basöz et al. 1999; EQE 2000). Therefore, a realistic and balanced classification scheme is a prerequisite for an effective vulnerability assessment of bridge stocks. The study presented herein addresses bridge types common in modern greek motorways, focussing on the bridges along the 680 km Egnatia Odos motorway that crosses Northern Greece from the Ionian Sea to the border with Turkey. For all practical purposes the bridge types found in Egnatia can be considered as representative of those recently or currently constructed in most European countries, particularly those in earthquake-prone areas.

Having established an appropriate classification scheme involving the most common bridge types (a total of 11), an analytical approach is proposed and used for deriving fragility curves, which are subsequently checked against empirical curves based on damage data from the US and Japan. In this approach, appropriate 3D models are set up of the generic bridges, representing each of the classes defined as discussed previously. The models are then analysed using the non-linear static (pushover) procedure, and the resistance (pushover) curves of the bridges are derived. Definition of damage states, an indispensable step in fragility curve development, is then made mainly in terms of parameters of the pushover curves of the generic bridges, and also utilising some local quantities like bearing deformation. An important feature of the study presented herein is that the procedure differentiates the way of defining damage according to the seismic energy dissipation mechanism in each bridge, i.e. bridges with yielding piers of the column type and bridges with bearings (with or without seismic links) and non-yielding piers of the wall type. Moreover, the activation of the abutment-backfill system due to closure of the gap between the deck and the abutment is also taken into account in deriving the fragility curves.

To the authors' best knowledge the sets of fragility curves presented herein constitute the most comprehensive such set for Europe, as far as the number of different typologies is concerned. This should not be construed as implying that similar or more sophisticated analytical procedures have not been used for deriving fragility curves for specific types of bridges in Europe (Monti and Nistico 2002; Erduran and Yakut 2004; Lupoi et al. 2005; Cardone et al. 2007), or elsewhere (Mander and Basöz 1999; Shinozuka et al. 2000; Hwang et al. 2000; Karim and Yamazaki 2001; Gardoni et al. 2003; Mackie and Stojadinovic 2007,

among several others). The development of the aforementioned broad set of fragility curves was possible due to the large number of research groups involved, which included teams mainly from the academic and research community, but also from professional engineering offices dealing with bridge design; all these teams worked using a basic common approach proposed by the Aristotle University of Thessaloniki group (Kappos et al. 2006) within the framework of a major research programme in Greece ('ASProGe: Seismic Protection of Bridges').

## 2 Classification of greek bridges

The starting points for the determination of a classification scheme for greek bridges were the corresponding schemes of ATC-13 (1985), NBI (FHWA 1995), those in the four editions of HAZUS (latest edition FEMA-NIBS 2004) and, to a lesser extent, the french classification scheme IQOA (SETRA 1998). After a critical review of the aforementioned classification systems, it was decided to develop a classification scheme based on the following bridge parameters, deemed as most significant regarding the seismic response:

1. Type of piers
2. Type of deck
3. Type(s) of pier-to-deck connection

For the aforementioned characteristics four, three and three classes are created, respectively, given in Tables 1, 2 and 3.

The combination of the above subclasses (Tables 1, 2 and 3) results in a total of 36 combinations, each denoted with a three-digit code; the first digit indicates the pier type, the second digit the deck type, and the third one the type of pier-to-deck connection. Following an initial screening of the existing bridges along the Egnatia Odos motorway it was found that out of

**Table 1** Classification of the piers (four types)

Code number	Description
1	Single column with cylindrical section
2	Single column with rectangular hollow section
3	Multi-column bent
4	Wall-type

**Table 2** Classification of the deck (three types)

Code number	Description
1	Slab (solid or with voids)
2	Box girder (single-cell section)
3	System with simply-supported precast-prestressed beams connected through continuous R/C top slab

**Table 3** Classification of the pier-to-deck connections (three types)

Code number	Description
1	Monolithic
2	Through bearings (with or without seismic isolation)
3	Combination of monolithic and bearing connections

**Table 4** Classification scheme for greek bridges

Code Number <sup>a</sup>	Description	Number of Bridges
111	Bridge with slab (solid or with voids) deck, monolithically connected to single column piers with cylindrical section	10–12
311	Bridge with slab (solid or with voids) deck, monolithically connected to multi-column bents	8–10
121	Bridge with box girder (single-cell) deck monolithically connected to single column piers with cylindrical section	6–8
221	Bridge with box girder (single-cell) deck monolithically connected to single column piers with rectangular hollow section	16–20
421	Bridge with box girder (single-cell) deck monolithically connected to wall-type piers	6–8
122	Bridge with box girder (single-cell) deck supported through bearings on single column piers with cylindrical section	5–7
422	Bridge with box girder (single-cell) deck supported through bearings on wall-type piers	5–6
232	Bridge with system with simply-supported precast-prestressed beams connected through continuous R/C slab supported through bearings on single column piers with rectangular hollow section	25–30
332	Bridge with system with simply-supported precast-prestressed beams connected through continuous R/C slab supported through bearings on multi-column bents	10–15
432	Bridge with system with simply-supported precast-prestressed beams connected through continuous R/C slab supported through bearings on wall-type piers	10–15
223	Bridge with box girder (single-cell) deck supported through combination of monolithic and bearing connections by single column piers with rectangular hollow section	10–15

<sup>a</sup> See Tables 1 to 3

the 36 possible classes, 27 actually exist. Then, among the 27 classes, those corresponding to 5 or more existing bridges were considered as “representative”. Hence, the final list of greek bridge classes considered in this study included the 11 classes shown in Table 4. It is worth pointing out that, by far, the most common category is the multi-span bridge with simply-supported precast-prestressed beams connected through a continuous R/C top slab (types 232, 332, and 432 in Table 4), a system that previous studies (e.g. Choi et al. 2004) indicate as the most vulnerable one in the concrete category (but less vulnerable than similar steel systems).

### 3 Procedure for deriving fragility curves

#### 3.1 Overview of proposed procedure

The methodology proposed here is based on non-linear static (pushover) analysis of the generic bridges, and is similar in some of its features to that adopted in HAZUS (Mander and Basöz 1999; FEMA-NIBS 2004). Damage states are defined mainly in terms of parameters of the pushover curves of the generic bridges, but also of some local quantities like shear deformation of the bearings. The key aspects of the proposed methodology are the following:

1. The bridges are classified into two main categories according to their seismic energy dissipation mechanism: bridges with yielding piers of the column type (monolithically connected to the deck or through a combination of bearings and monolithic connections which is common to modern ravine bridges in Europe) and bridges with bearings (with or without seismic links, like stoppers) and non-yielding piers of the wall type. In the former type of bridges the inelastic behaviour is developed due to the formation of plastic hinges at the pier base (and the top, if the pier-to-deck connection allows the development of substantial bending moment), while in the latter type inelastic behaviour develops due to the inelastic behaviour of bearings (and seismic links), because in most cases the deck is supported by wall-type piers which remain in the elastic range even for strong earthquake events. A key difference between the two main categories is the shape of the pushover curve (the starting point for the derivation of fragility curves according to the proposed procedure), which is clearly bilinear in the first category and essentially linear in the second one (slope defined by the effective stiffness of the bearings), as will be shown in the next section. Note that in Table 4 bridges 422 and 432 belong to the ‘bearings/non-yielding piers’ category, while the rest to the ‘yielding piers’ category.
2. Damage states are defined using damage parameters instead of damage indices. The use of damage parameters for the derivation of fragility curves is advantageous against the use of damage indices (% of damage in the structure), given that the threshold of the first damage state (DS1-Minor/Slight damage) is expressed as a specific value of the damage parameter (e.g. displacement), whereas in terms of damage indices it corresponds to any non-zero value. The damage parameter used in the proposed methodology is the displacement  $d$  of the bridge deck derived on the basis of a specific criterion determined for each damage state depending on the bridge energy dissipation mechanism (inelastic piers or bearings), as discussed in more detail in Sect. 3.3.
3. Possible damage due to the activation of the abutment-backfill system is also taken into account in the longitudinal direction of bridges because of the closure of the gap between the deck and the abutments; it is noted here that all modern bridges in Greece have abutments of the seat-type with a longitudinal joint to compensate for temperature, creep and shrinkage effects, as well as part of the design seismic displacement (40% according to the current greek code). This is a major issue arising typically during the assessment of the bridge’s seismic response in the longitudinal direction (gaps in the transverse direction are far less common). In the case of short bridges (such as overpasses) the abutment-backfill contribution is significant also in the transverse direction and was modelled where appropriate. During the design of the bridge these aspects are usually disregarded under the (implicit) assumption that the response of the bridge subsequent to gap closure will not be worse than that before closure; hence, in the analysis of the bridge the support of the deck at the abutments is considered either as longitudinally free or through a spring support, the stiffness of the spring derived from the shear stiffness of the bearings, if elastomeric bearings are used, as is commonly the case in Greece and elsewhere. Since only part of the seismic displacement is taken into account when designing the longitudinal joint, in bridges where non-seismic (environmental etc.) displacements are relatively small, during the design earthquake event the gap at the abutment will close, resulting into collision of the back-wall of the abutment and the ensuing significant redistribution of seismic forces between piers and the abutment-backfill system, which may lead to its failure (vertical and/or lateral offsets, foundation failure, settlement of backfill, and so on).

The successive steps of the proposed methodology are described in the following sections.

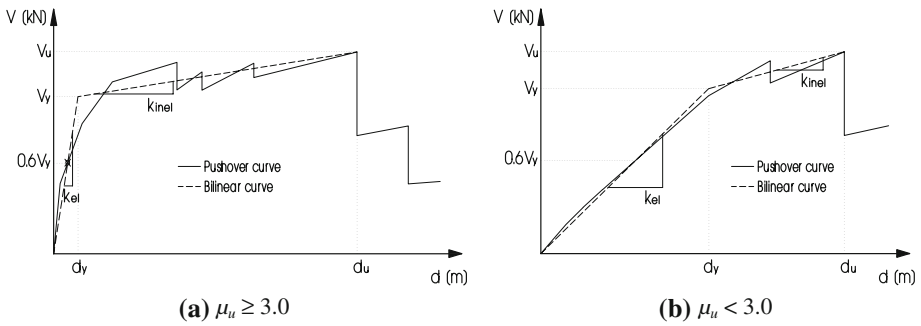


**Fig. 1** Pushover curves and their bilinear idealization. (a)  $\mu_u \geq 3.0$ , (b)  $\mu_u < 3.0$

### 3.2 Derivation of pushover and capacity curves

In bridges with yielding piers of the column type, pushover curves, i.e. plots of base shear versus displacement of the ‘monitoring’ point on the deck (taken as the one above the critical pier or abutment) are derived by performing a standard (fundamental mode based) pushover analysis. Some of the bridges have also been analysed using a modal pushover analysis for each mode independently (Paraskeva et al. 2006). When the modal pushover method is used, a “multi-modal” curve can be constructed by an appropriate combination of the values from individual curves (Paraskeva and Kappos 2007); however, to retain uniformity along all typologies studied, such multi-modal curves are not used herein. Reinforced concrete members are modelled using the point hinge model of SAP2000 (CSI 2005) with multilinear moment—rotation law for each hinge, accounting for residual strength after exceeding the rotational capacity; relevant details are given in Kappos et al. (2007).

The derived pushover curve is then idealized as a bilinear one (Fig. 1) in order to define a conventional yield displacement,  $d_y$  and ultimate displacement  $d_u = \mu_u \cdot d_y$ , both referring to the entire bridge, not to a single pier ( $d_u$  corresponds to more than 20% drop in the base shear capacity). When the available displacement ductility ratio is relatively large ( $\mu_u \geq 3.0$ , bridges with monolithic pier-to-deck connections) the pushover curve has the shape of Fig. 1a, while in the case of bridges with relatively low ductility ( $\mu_u < 3.0$ , bridges with deck supported on the piers through bearings) the pushover curve has the shape of Fig. 1b.

In the case of bridges with bearings (with or without seismic links) and non-yielding piers of the wall type, pushover curves are derived by performing a standard pushover analysis given that the first (fundamental) mode of the bridge is similar to the first (fundamental) mode of the deck since the wall-type piers are much stiffer than the bearings, and as a consequence has a significant participating mass ratio. In the longitudinal direction the first mode of the deck is a rigid-body displacement, while in the transverse direction it has a sinusoidal shape or it consists of a rigid-body displacement and rotation, depending on whether the transverse displacement of the deck at the abutments is restrained or not. In addition, the derived pushover curve has already a bilinear shape because of the corresponding bilinear behaviour of the bearings and, as a consequence, there is no need for bilinear idealization (Fig. 2a, b-dashed line). Whenever seismic links (stoppers) are present, the pushover curve has a similar shape but an apparent hardening/softening is noticed, due to the successive activation and failure, respectively, of seismic links (Fig. 2b-continuous line). Furthermore, in the case of common elastomeric bearings the bilinear behaviour may be represented by a

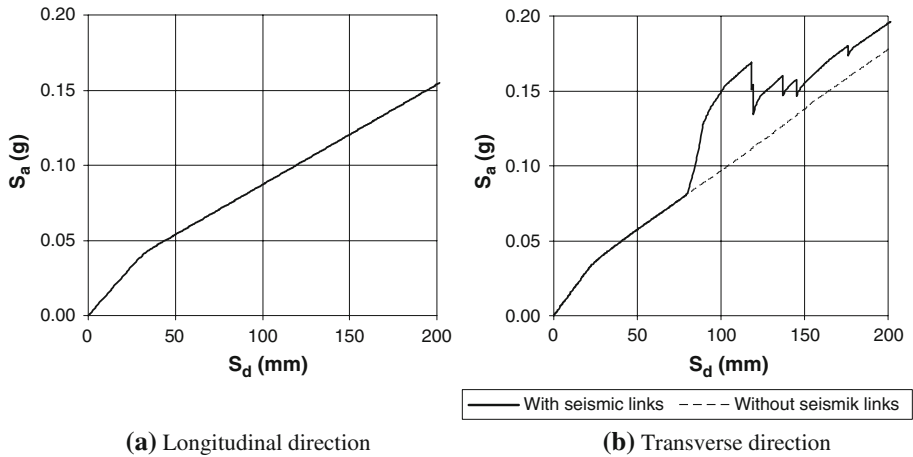


**Fig. 2** Capacity curves of a bridge with bearings and non-yielding piers. **(a)** Longitudinal direction, **(b)** Transverse direction

simple quasi-elastic (linear) behaviour given that the hysteresis loop of these bearings is very thin (low equivalent damping ratio,  $\zeta \approx 5\%$ ). This choice is advisable for both the economy of the analysis procedure and for the more accurate assessment of the target displacement, since the definition of the first branch of the bilinear diagram of the bearings is subject to uncertainties.

As noted previously, the activation of the abutment-backfill system due to closure of the gap between the deck and the abutments may strongly affect the damage mechanism. So, a “full-range” analysis of the bridge is suggested in order to model the response of the bridge subsequent to gap closure; a detailed finite element modelling of the abutment-backfill system (in both the longitudinal and the transverse direction), including soil flexibility (non-linear behaviour and consideration of both stiff and soft soils) and pile non-linearity (in flexure and shear), was made in the case of bridge 111 (Kappos et al. 2007). In such an analysis, all stages of the bridge seismic response are studied, i.e. the initial stage when the joint is still open, during which the contribution of the abutment-backfill system is small, and the second stage after closure, during which a significant redistribution of seismic forces between the piers and the abutment-backfill system takes place. In this case the pushover curve has a quadrilinear shape (Fig. 3) and the additional parameters that have to be defined are the displacement at yielding and at failure of the abutment-backfill system,  $d_{y, ab}$  and  $d_{u, ab}$ , respectively.

The derived pushover curves are converted to capacity curves, i.e. in spectral acceleration versus spectral displacement format, in order to be superimposed on the same diagram with the demand spectrum for the application of the capacity spectrum method (ATC 1996). Clearly, other methods for determining the displacement demand can also be used within the framework of the proposed procedure.

### 3.3 Definition of damage states

In line with Basöz et al. (1999), wherein analytical fragility curves were calibrated against empirical ones obtained from actual bridge damage data, four damage states are considered in addition to the no-damage state (DS0): minor/slight (DS1), moderate (DS2), major/extensive

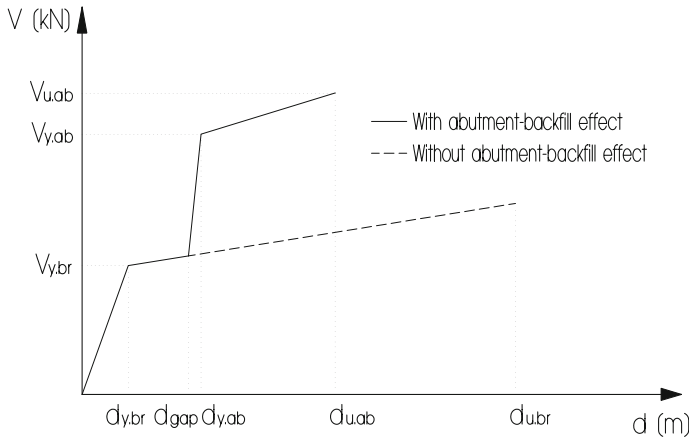


**Fig. 3** Capacity curve when longitudinal gap closure is modelled

**Table 5** Definition of damage states for bridges with inelastic piers of the column type – Full-range analysis in the longitudinal direction

Damage state	Required interventions	Threshold values of $d$	
		Longitudinal direction	Transverse direction
DS0 None	None	$\leq \min\{0.7 \cdot d_{y,br}, d_{gap}\}$	$\leq 0.7 \cdot d_{y,br}$
DS1 Minor/slight	Inspect, adjust, patch	$> \min\{0.7 \cdot d_{y,br}, d_{gap}\}$	$> 0.7 \cdot d_{y,br}$
DS2 Moderate	Repair components	$> \min\{1.5 \cdot d_{y,br}, d_{y,br} + (1/3) \cdot (d_{u,br} - d_{y,br}), d_{y,ab} + (1/3) \cdot (d_{u,ab} - d_{y,ab})\}$	$> \min\{1.5 \cdot d_{y,br}, d_{y,br} + (1/3) \cdot (d_{u,br} - d_{y,br})\}$
DS3 Major/extensive	Rebuild components	$> \min\{3.0 \cdot d_{y,br}, d_{y,br} + (2/3) \cdot (d_{u,br} - d_{y,br}), d_{y,ab} + (2/3) \cdot (d_{u,ab} - d_{y,ab})\}$	$> \min\{3.0 \cdot d_{y,br}, d_{y,br} + (2/3) \cdot (d_{u,br} - d_{y,br})\}$
DS4 Failure/collapse	Rebuild bridge	$> \min\{d_{u,br}, d_{u,ab}\}$	$> d_{u,br}$

(DS3) damage, and failure/collapse (DS4). The damage states are defined using the displacements of the bridge  $d$ , at characteristic points on the derived pushover curve.

The two directions of the bridge are examined separately. In the case of bridges with yielding piers of the column type (Tables 5 and 6) the definition of damage states is based on combining experience from buildings with the limited information available for bridges (Choi et al. 2004; Erduran and Yakut 2004). The damage suffered by the bridge is defined directly on the corresponding pushover curve as a function of the yield and the ultimate displacement (see Fig. 1),  $d_{y,br}$  and  $d_{u,br}$ , respectively (Table 5). The first damage state, DS1 (minor/slight damage), is defined as a function of the yield displacement,  $d_{y,br}$ , while the definition of the last one (DS4, failure) is based on the ultimate displacement of the bridge,  $d_{u,br}$ . Damage states DS2 (moderate damage) and DS3 (major/extensive) are defined on the basis of the post-yielding branch of the derived pushover curve. In the case of bridges with  $\mu_u \geq 3.0$  the threshold values are constant,  $\mu = 1.5$  and  $3.0$ , respectively, while for bridges with  $\mu_u < 3.0$  the threshold values are  $d_{y,br} + 1/3(d_{u,br} - d_{y,br})$  and  $d_{y,br} + 2/3(d_{u,br} - d_{y,br})$ , respectively.



**Table 6** Definition of damage states for bridges with inelastic piers of the column type—Approximate analysis in the longitudinal direction

Damage state	Required interventions	Threshold values of $d$	
		Longitudinal direction	Transverse direction
DS0 None	None	$\leq \min\{0.7 \cdot d_{y,br}, d_{gap}\}$	$\leq 0.7 \cdot d_{y,br}$
DS1 Minor/slight	Inspect, adjust, patch	$> \min\{0.7 \cdot d_{y,br}, d_{gap}\}$	$> 0.7 \cdot d_{y,br}$
DS2 Moderate	Repair components	$> \min\{1.5 \cdot d_{y,br}, d_{y,br} + (1/3) \cdot (d_{u,br} - d_{y,br}), 1.1 \cdot d_{gap}\}$	$> \min\{1.5 \cdot d_{y,br}, d_{y,br} + (1/3) \cdot (d_{u,br} - d_{y,br})\}$
DS3 Major/extensive	Rebuild components	$> \min\{3.0 \cdot d_{y,br}, d_{y,br} + (2/3) \cdot (d_{u,br} - d_{y,br}), 1.2 \cdot d_{gap}\}$	$> \min\{3.0 \cdot d_{y,br}, d_{y,br} + (2/3) \cdot (d_{u,br} - d_{y,br})\}$
DS4 Failure/collapse	Rebuild bridge	$> \begin{cases} d_{u,br}, & \text{for } d_{u,br} < 1.1 \cdot d_{DS3} \\ \max\{a \cdot d_{u,br}, 1.1 \cdot d_{DS3}\} \end{cases}$	$> d_{u,br}$

In the longitudinal direction and in order to take into account the abutment-backfill effect, additional parameters are defined. In particular, when the pushover curve is derived by a “full-range” analysis (Fig. 3; Table 5) the first damage state (DS1) is defined as a function, not only of  $d_y$ , but also of the displacement at gap closure,  $d_{gap}$ , in order to take into account the initial activation of the abutment-backfill system. The definition of the second and the third damage state (DS2 and DS3) is similar to the corresponding definitions for the bridge without abutment-backfill effect, and is based on the post-yielding branch of the pushover curve after the activation of the abutment-backfill system. The additional threshold values (minimum value governs, see Table 5) are  $d_{y,ab} + (1/3) \cdot (d_{u,ab} - d_{y,ab})$ , and  $d_{y,ab} + (2/3) \cdot (d_{u,ab} - d_{y,ab})$ , respectively. Finally, the last damage state (DS4) is defined introducing an additional criterion related to the ultimate displacement after failure of the abutment-backfill system,  $d_{u,ab}$  (see Fig. 3). In the more common in design practice case that the analysis of the bridge is performed ignoring the abutment-backfill effect, approximate threshold values are suggested. The first damage state (DS1) is defined as before, i.e. by the displacement at gap closure,  $d_{gap}$ . For damage states DS2 and DS3, the additional threshold values are  $1.1 \cdot d_{gap}$  and  $1.2 \cdot d_{gap}$ , respectively. The threshold value for the last damage state is defined as the maximum of  $a \cdot d_{u,br}$  ( $a < 1$ ) and  $1.1 \cdot d_{DS3}$ . The suggested value for  $a$  is 0.6 (Kappos et al. 2007). Both the aforementioned expressions are approximations of the displacement at failure of the abutment-backfill system.

In the case of bridges with bearings (with or without seismic links) and non-yielding piers of the wall type, four damage states can be considered, as before, (DS1: Minor/Slight damage, DS2: Moderate damage, DS3: Major/Extensive damage, and DS4: Failure/Collapse), after the no-damage state (DS0). The definition of these damage states is based on the shear deformation of the single bearing,  $\gamma_{bi}$  (Table 7). These threshold values refer to common elastomeric bearings and resulted on the basis of limited test data from manufacturers, supplemented by code values and engineering judgment. Given the values for the single bearing at each damage state, the total shear deformation of all bridge bearings is calculated as their average shear deformation, using the following relationship:

$$\gamma_{tot} = \frac{\sum_{i=1}^N \gamma_{bi}}{N} \tag{1}$$

**Table 7** Definition of damage states for the single bearing and the total number of bridge bearings

Damage state		Damage state limits $\gamma_{bi}, \gamma_{tot}$	Threshold values $\gamma_{bi}, \gamma_{tot}$
DS0	None	$0 \leq \gamma_{bi}, \gamma_{tot} < \gamma_y = 0.2$	$\leq \gamma_y = 0.2$
DS1	Minor/slight	$\gamma_y = 0.2 \leq \gamma_{bi}, \gamma_{tot} < 1.5$	$> \gamma_y = 0.2$
DS2	Moderate	$1.5 \leq \gamma_{bi}, \gamma_{tot} < 2.0$	$> 1.5$
DS3	Major/extensive	$2.0 \leq \gamma_{bi}, \gamma_{tot} < 5.0$	$> 2.0$
DS4	Failure/collapse	$\gamma_{bi}, \gamma_{tot} \geq 5.0$	$> 5.0$

**Table 8** Definition of damage states for bridges with bearings and non-yielding piers of the wall type—Full-range analysis in the longitudinal direction

Damage state		Threshold values $d$	
		Longitudinal direction	Transverse direction
DS0	None	$\leq \min\{d(\gamma_{tot} = \gamma_y = 0.2), d_{gap}\}$	$\leq d(\gamma_{tot} = \gamma_y = 0.2)$
DS1	Minor/slight	$> \min\{d(\gamma_{tot} = \gamma_y = 0.2), d_{gap}\}$	$> d(\gamma_{tot} = \gamma_y = 0.2)$
DS2	Moderate	$> \min\{d(\gamma_{tot} = 1.5), d_{y,ab} + (1/3) \cdot (d_{u,ab} - d_{y,ab})\}$	$> d(\gamma_{tot} = 1.5)$
DS3	Major/extensive	$> \min\{d(\gamma_{tot} = 2.0), d_{y,ab} + (2/3) \cdot (d_{u,ab} - d_{y,ab})\}$	$> d(\gamma_{tot} = 2.0)$
DS4	Failure/collapse	$> \min\{d(\gamma_{tot} = 5.0), d_{u,ab}\}$	$> d(\gamma_{tot} = 5.0)$

where  $\gamma_{bi}$  is the shear deformation of the single bearing and  $N$  is the total number of bridge bearings. The definitions of damage states for the entire bridge according to the total shear deformation  $\gamma_{tot}$ , are similar to the corresponding definitions for the single bearing (Table 7).

The damage states for the entire bridge are defined separately for the two directions, as in the case of bridges with yielding piers of the column type. In the transverse direction the definition of damage states is based on the bridge displacements  $d_{DSi}$  corresponding to the threshold values for the average shear deformation (Eq. 1),  $\gamma_{tot}$  (see Table 7). In the longitudinal direction the damage states are defined according to both the bridge displacements  $d_{DSi}$ , as defined for the transverse direction, and the additional parameters accounting for the abutment-backfill effect, as defined in the case of bridges with yielding piers of the column type.

### 3.4 Estimation of fragility curve parameters

In line with other similar procedures (FEMA-NIBS 2004; Mackie and Stojadinovic 2007), fragility curves in the proposed methodology are expressed by the lognormal probability distribution function:

$$P_f(DP \geq DP_i | S) = \Phi \left[ \frac{1}{\beta_{tot}} \cdot \ln \left( \frac{S}{S_{mi}} \right) \right] \tag{2}$$

where  $P_f(\cdot)$  is the probability of the damage parameter  $DP$  being at, or exceeding, the value  $DP_i$  for the  $i$ th damage state (Tables 5, 6, 8 and 9) for a given seismic intensity level defined by the earthquake parameter  $S$  (Peak Ground Acceleration- $PGA$ , Spectral Acceleration- $S_a$ , or Spectral Displacement- $S_d$ ),  $\Phi$  is the standard cumulative probability function,  $S_{mi}$  is the median threshold value of the earthquake parameter  $S$  required to cause the  $i$ th damage state, and  $\beta_{tot}$  is the total lognormal standard deviation.

The description of the fragility curve according to Eq. 2 involves only two parameters,  $S_{mi}$  and  $\beta_{tot}$ . The first parameter is estimated on the basis of the capacity spectrum method,

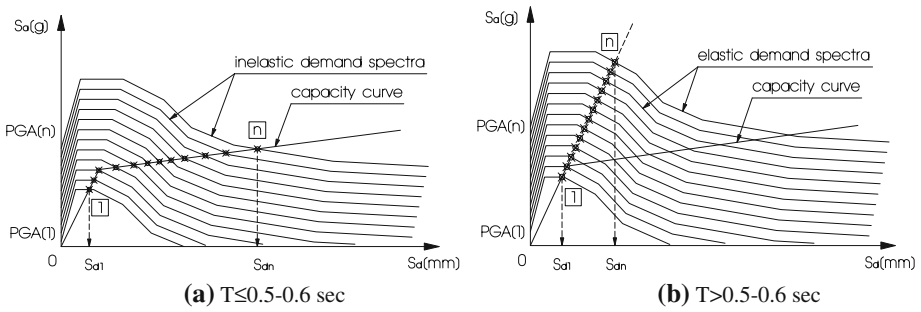


**Fig. 4** Capacity spectrum method. (a)  $T \leq 0.5\text{--}0.6$  s, (b)  $T > 0.5\text{--}0.6$  s

**Table 9** Definition of damage states for bridges with bearings and non-yielding piers of the wall type—Approximate analysis in the longitudinal direction

Damage state		Threshold values $d$	
		Longitudinal direction	Transverse direction
DS0	None	$\leq \min\{d(\gamma_{tot} = \gamma_y = 0.2), d_{gap}\}$	$\leq d(\gamma_{tot} = \gamma_y = 0.2)$
DS1	Minor/slight	$> \min\{d(\gamma_{tot} = \gamma_y = 0.2), d_{gap}\}$	$> d(\gamma_{tot} = \gamma_y = 0.2)$
DS2	Moderate	$> \min\{d(\gamma_{tot} = 1.5), 1.1 \cdot d_{gap}\}$	$> d(\gamma_{tot} = 1.5)$
DS3	Major/extensive	$> \min\{d(\gamma_{tot} = 2.0), 1.2 \cdot d_{gap}\}$	$> d(\gamma_{tot} = 2.0)$
DS4	Failure/collapse	$> \begin{cases} d(\gamma_{tot} = 5.0), & \text{for } d(\gamma_{tot} = 5.0) < 1.1 \cdot d_{DS3} \\ \max\{a \cdot d(\gamma_{tot} = 5.0), 1.1 \cdot d_{DS3}\} \end{cases}$	$> d(\gamma_{tot} = 5.0)$

wherein the demand spectrum is plotted for a range of values of the earthquake parameter  $S$  (in spectral acceleration versus spectral displacement format) and it is superimposed on the same plot with the capacity curve of the bridge (Fig. 4). The earthquake parameter used in this study is the peak ground acceleration (PGA). Figure 4a shows the general case of the capacity spectrum method combined with inelastic demand spectra (Fajfar 1999), while Fig. 4b shows the case wherein the fundamental period  $T$  of the bridge is longer than about 0.5–0.6 s, i.e. the range of periods wherein the equal displacement approximation is a reasonable assumption. It is worth noting that in the case of a “full-range” analysis wherein the pushover curve has a quadrilinear shape, the capacity spectrum method should be applied for an equivalent bilinear shape due to the lack of research results on inelastic spectra for quadrilinear behaviour.

Using the intersection points of these curves (Fig. 4) the damage versus earthquake parameter diagram (Fig. 5) can be plotted, which represents the evolution of damage parameter  $DP$  with increasing earthquake intensity (PGA in this case). Then, using the damage versus earthquake parameter diagram and the definitions of Tables 5, 6, 8 and 9, the median threshold value of the earthquake parameter  $S_{mi}$  can be obtained for each damage state. For example the threshold value for the second damage state (DS2: Moderate damage) in the transverse direction of a bridge with yielding piers of the column type is that corresponding to  $\min\{1.5 \cdot d_{y, br}, d_{y, br} + (1/3) \cdot (d_{u, br} - d_{y, br})\}$  (Tables 5, 6), while in the case of a bridge with bearings and non-yielding piers of the wall type, it is that corresponding to  $d(\gamma_{tot} = 1.5)$  (Tables 8, 9).

The second parameter of Eq. 2 is the total lognormal standard deviation  $\beta_{tot}$ , which takes into account the uncertainties in seismic input motion (demand), in the response and resistance

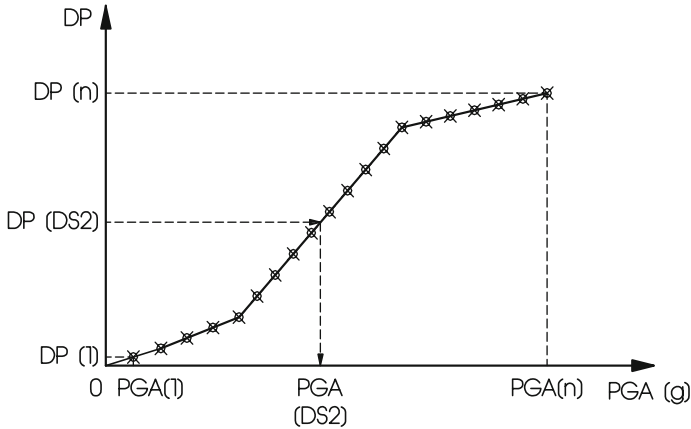


**Fig. 5** Evolution of damage with earthquake parameter

of the bridge (capacity), and in the definition of damage states. This parameter ( $\beta_{tot}$ ) can be estimated by a statistical combination of the individual uncertainties (in demand, capacity, and damage state definition) assuming these are statistically independent. The value of  $\beta_{tot}$  was calibrated by [Dutta and Mander \(1998\)](#) using a theoretical approach and validated on the basis of empirical fragility curves obtained from actual bridge damage data gathered from the Loma Prieta (1989) and Northridge (1994) earthquakes. According to these studies the value of  $\beta_{tot}$  was set to 0.6; due to the lack of a more accurate estimation of uncertainties in capacity, demand and damage states,  $\beta_{tot} = 0.6$  was used in the present study, but clearly more work is needed in this direction.





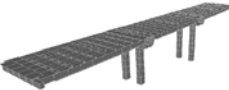
#### 4 Derivation of fragility curves for greek bridges

The selection of bridges for the application of the proposed methodology was based on the classification scheme for greek bridges (see Sect. 2). Thus, 11 bridges along the Egnatia Odos motorway were selected, one from each class of Table 4. The main characteristics of the selected bridges are given in Table 10; recall that in the ID code of each bridge the first digit refers to the pier type (Table 1), the second to the deck type (Table 2), and the third to the pier-deck connection type (Table 3).

##### 4.1 Fragility curves using the proposed method

The sets of fragility curves derived for each of the 11 bridges using the elastic spectrum of the 2003 Greek Seismic Code (which is very similar to that of the 1994 ENV Eurocode 8), as demand spectrum, are given in Figs. 6–16. It is pointed out that for all bridges a 3D model has been set up, and analysis has been carried out for both the longitudinal and transverse direction. In most of the analyses the SAP 2000 Non-linear software package ([CSI 2005](#)) has been used, and every effort has been made for all research teams to use the same modelling assumptions. Nevertheless, only one set of analyses (see [Kappos et al. 2007](#)) was carried out with explicit modelling of the closure of the end joints and the ensuing activation of the abutment-backfill system, while the other sets of analyses were carried out assuming continuously open joints at the abutments, and fragility curves in the longitudinal direction were

**Table 10** Main characteristics of the bridges selected for each class

Structural configuration	Bridge name and class*	No. of spans	Span length	Total length	Pier-to-deck connection	Curvature	Foundation
	Pedini Bridge 111	3	19.0+ 32.0+ 19.0	70.0	monolithic	in height	pile groups
	Siatista Bridge 311	3	16.25+ 30.5+ 16.25	63.0	monolithic	minor curvature in plan	pile groups
	T7 (Section 14.1.2) bridge 121	3	27.0+ 45.0+ 27.0	99.0	monolithic	no	footings
	G11 bridge (right branch) 221	3	64.3+ 118.6+ 64.3	247.2	monolithic	in plan	caissons
	G9 (Section 5.1) Bridge 421	2	85.0	170.0	monolithic	in plan	caissons
	Eirini Bridge 122	4	45.0	180.0	through bearings	no	pile groups
	Lissos River Bridge 422	11	1×29.56+ 3×37.05+ 6×44.35+ 1×26.50	433.31	through bearings	no	pile groups
	2 <sup>nd</sup> Kavala Ravine Bridge 232	4	42.0+ 2×43.5+ 42.0	180.0	through bearings	no	caissons
	G2 (Section 1.1.6) Bridge 332	3	30.7+ 31.7+ 30.7	93.1	through bearings	no	pile groups
	Kossynthos River Bridge 432	5	35.0+ 3×36.0+ 35.0	178.0	through bearings	no	pile groups
	Krystallopigi Bridge 223	12	44.17+ 10×54.98+ 44.17	638.19	monolithic/ through bearings	in plan	pile groups

\* See Tables 1 to 4

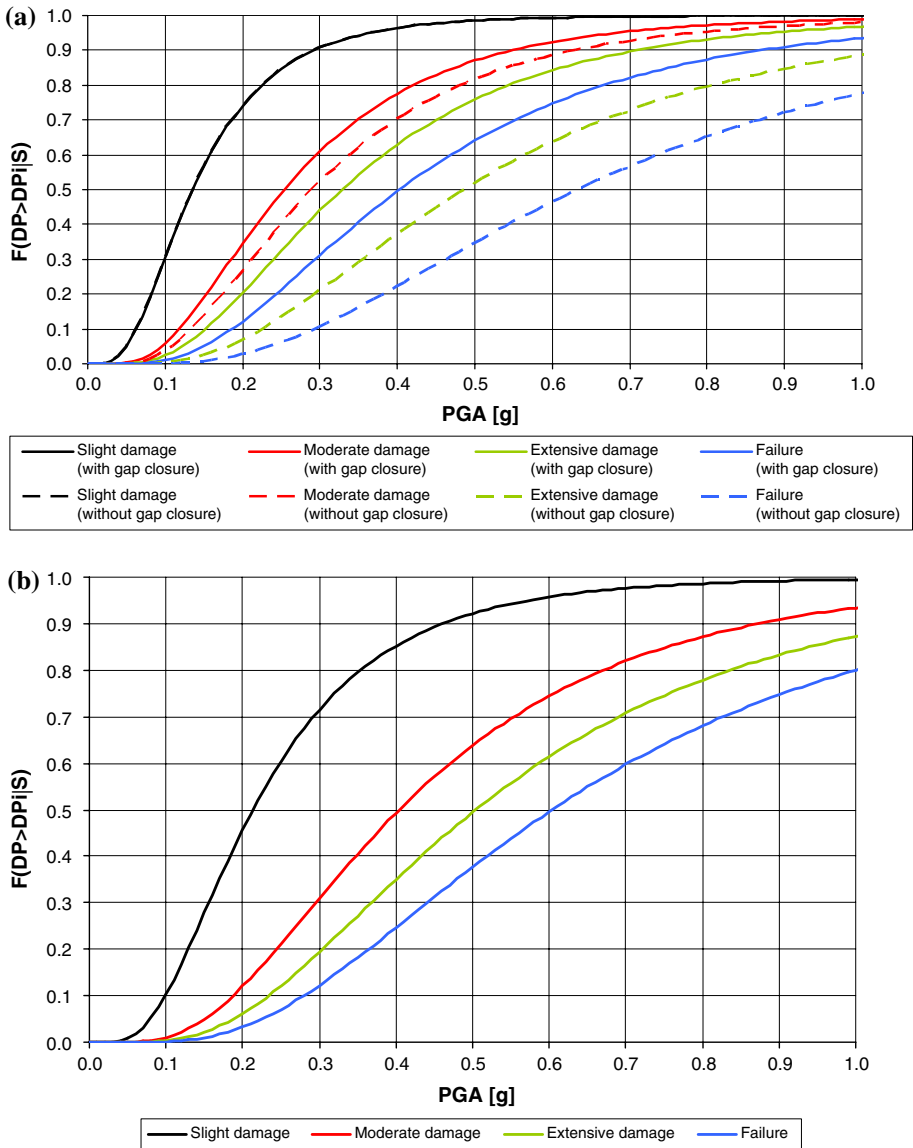


**Fig. 6** Fragility curves of Pedini bridge. (a) Longitudinal direction, (b) Transverse direction

derived based on the simplified criteria (that estimate the yield and ultimate deformation of the abutment system in terms of that of the longitudinally unrestrained deck system) given in Tables 6 and 9 for the two main categories of bridges considered in this study. For comparison purposes, the fragility curves resulting from ignoring joint closure are also given (dotted lines in Figs. 6a–16a) for the longitudinal direction of the bridges.

Referring to the 22 sets of fragility curves (11 bridges  $\times$  2 directions), and the additional 11 sets for the longitudinal direction (ignoring joint closure) in Figs. 6–16, several observations can be made. In the case of bridges with yielding piers of the column type, comparing

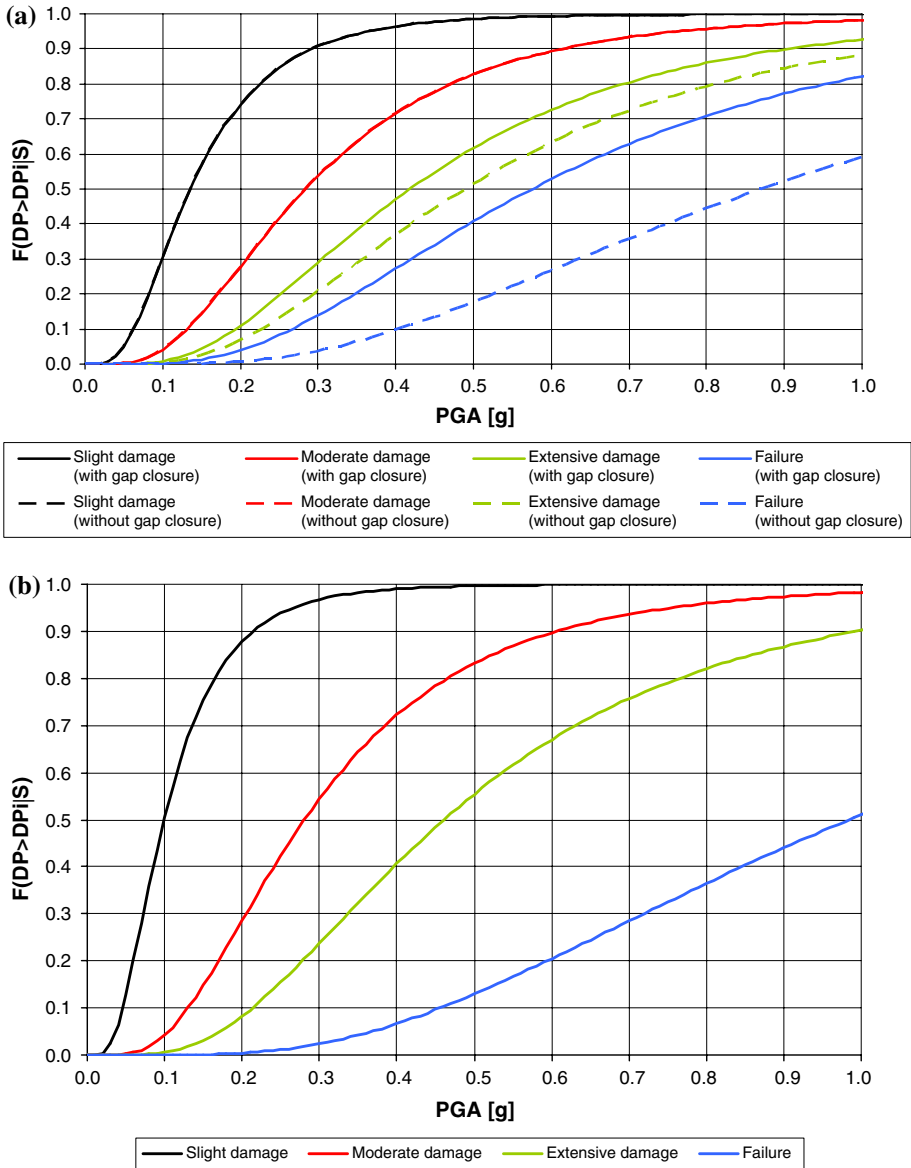


**Fig. 7** Fragility curves of Siatista bridge. (a) Longitudinal direction, (b) Transverse direction

the derived sets of fragility curves in the transverse and longitudinal direction without taking into account the abutment-backfill effect, it is observed that the distance between the last damage state (DS4: Failure/Collapse) and the remaining three damage states increases according to the available ductility of the bridge (e.g. compare T7 bridge and Krystallopigi bridge). In the case of bridges with bearings and non-yielding piers of the wall type, the distance between the two intermediate damage states DS2 and DS3 is small (see Lissos and Kossynthos bridges), reflecting the small difference between the corresponding threshold values of  $\gamma_{tot}$ , 1.5 and 2.0, respectively (Table 7). Furthermore, when the deck moves as

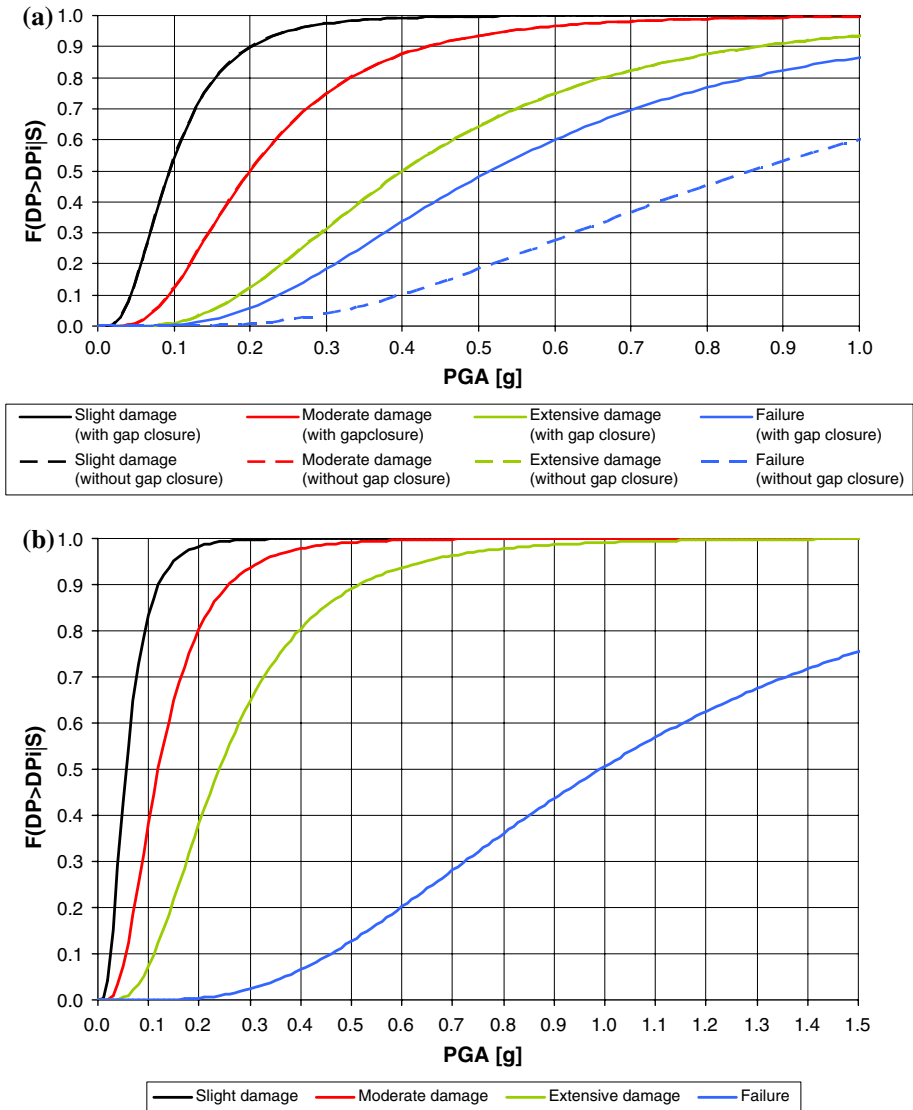


**Fig. 8** Fragility curves of T7 bridge. (a) Longitudinal direction, (b) Transverse direction

a rigid body (e.g. Kossynthos bridge) the probability of being in, or exceeding, a specific damage state for a given earthquake intensity is greater than in the case wherein the transverse deformation of the deck has a sinusoidal shape (Lissos bridge) due to the restraint of transverse displacement at the abutments; this is expected from the definition of  $\gamma_{tot}$  (Eq. 2), since in the latter case the shear deformation of the bearings reduces towards the abutments.

Comparing the fragility curves derived for the various classes, it is noted that apart from the expected similarities in the fragility curves, reflecting the corresponding similarities in the seismic response of bridges designed to similar code provisions, there are also many differences, even between ostensibly similar classes due to differences in either geometric



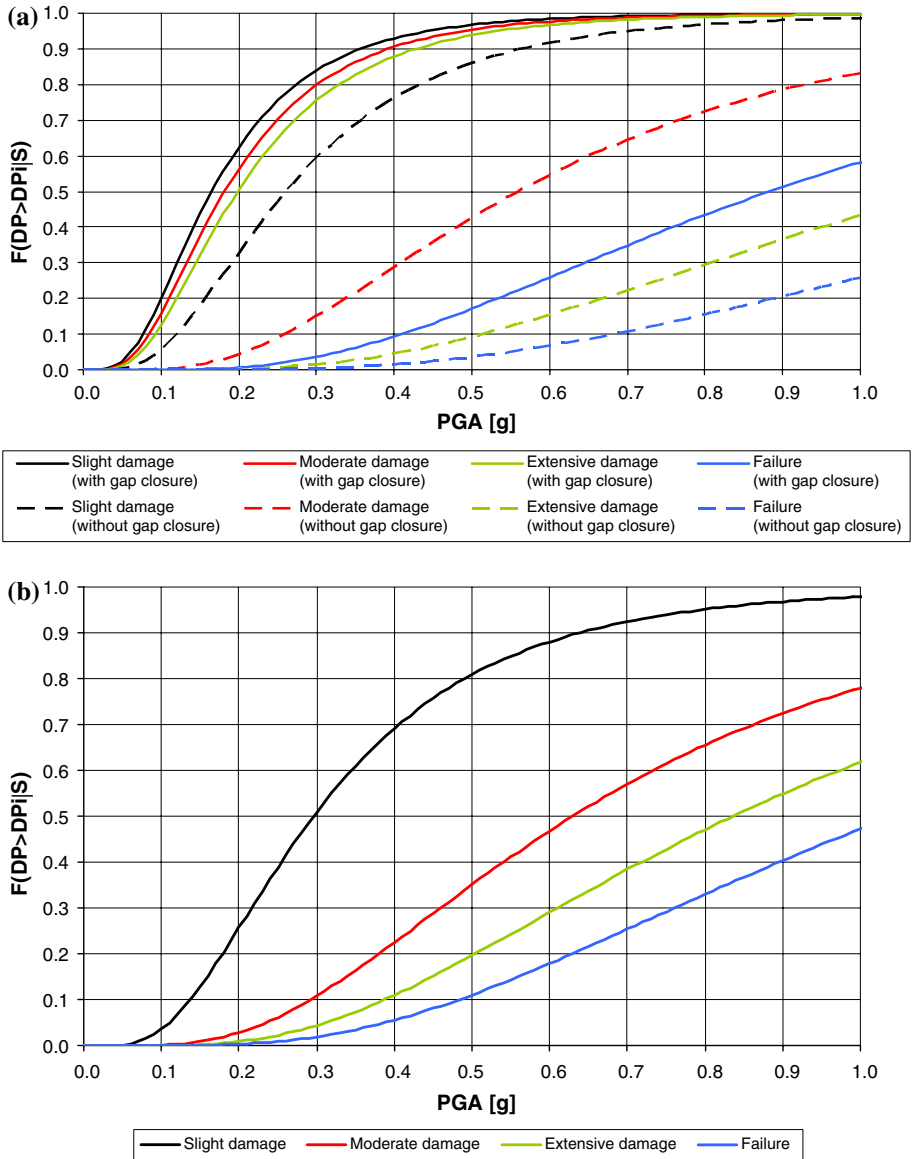


**Fig. 9** Fragility curves of G11 bridge. (a) Longitudinal direction, (b) Transverse direction

characteristics (span lengths, pier heights) or pier-deck connections, all of which can vary significantly among bridges with similar structural system.

Another interesting issue is the comparison between the two bridge directions, in particular the attempt to identify a consistently weaker direction, which, if actually existed, would significantly reduce the effort for deriving fragility curves, since only one set of analyses would be required. The present study shows that the critical direction is the longitudinal (as anticipated by members of the research team with experience in bridge design) if the definition of the critical direction is based on damage states DS3 and DS4 (i.e. the higher

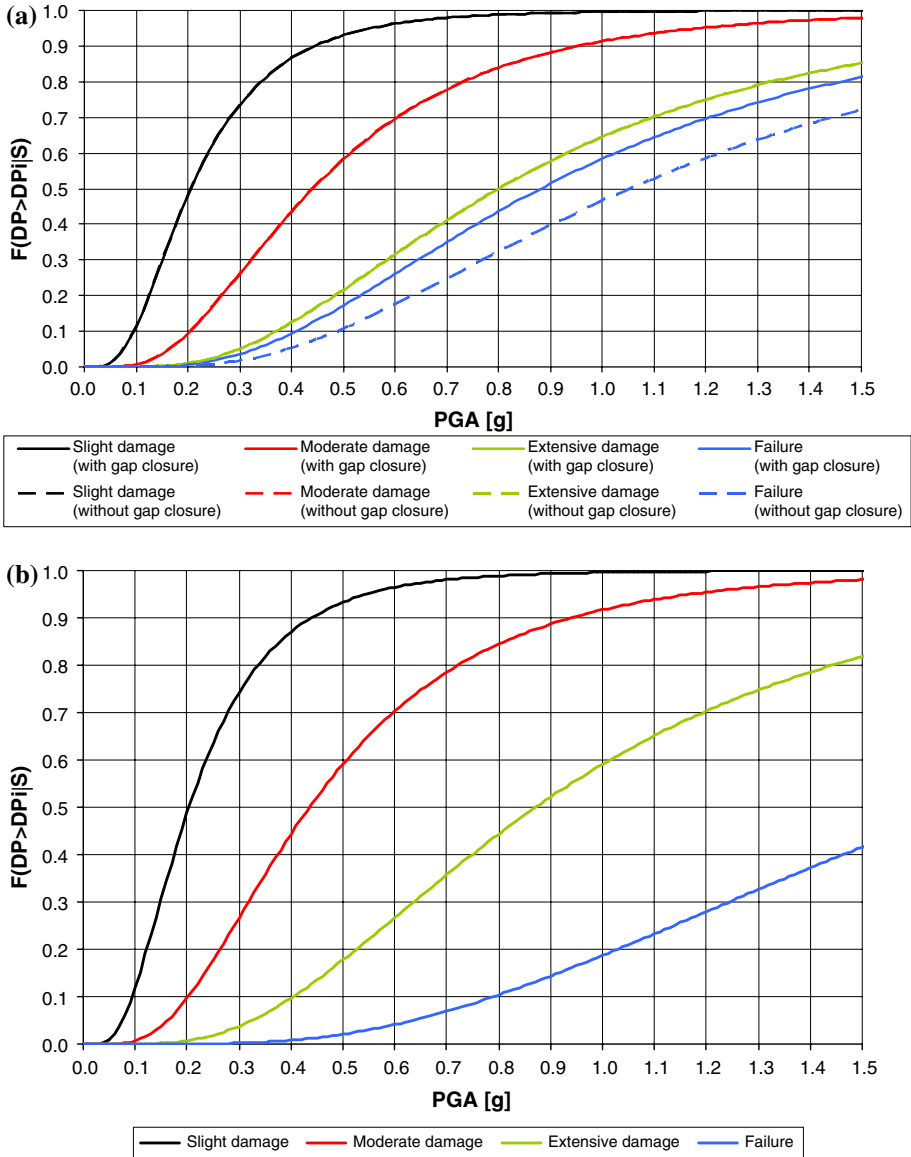


**Fig. 10** Fragility curves of G9 bridge. (a) Longitudinal direction, (b) Transverse direction

two states). This conclusion is valid under the assumption that in the transverse direction a ‘standard’ pushover analysis is performed i.e. a load profile following the fundamental bridge mode is applied. It has been found (Paraskeva et al. 2006) that this profile does not necessarily provide critical values for all response quantities. The key reasons for the longitudinal direction being the critical one are first because the strength of the bridge is smaller in this direction due to the orientation of the bridge piers (their major axis is normal to the bridge axis, the exception being single-column cylindrical piers that have the same strength in every direction), and the second one that the gap between the deck and the bridge abutments

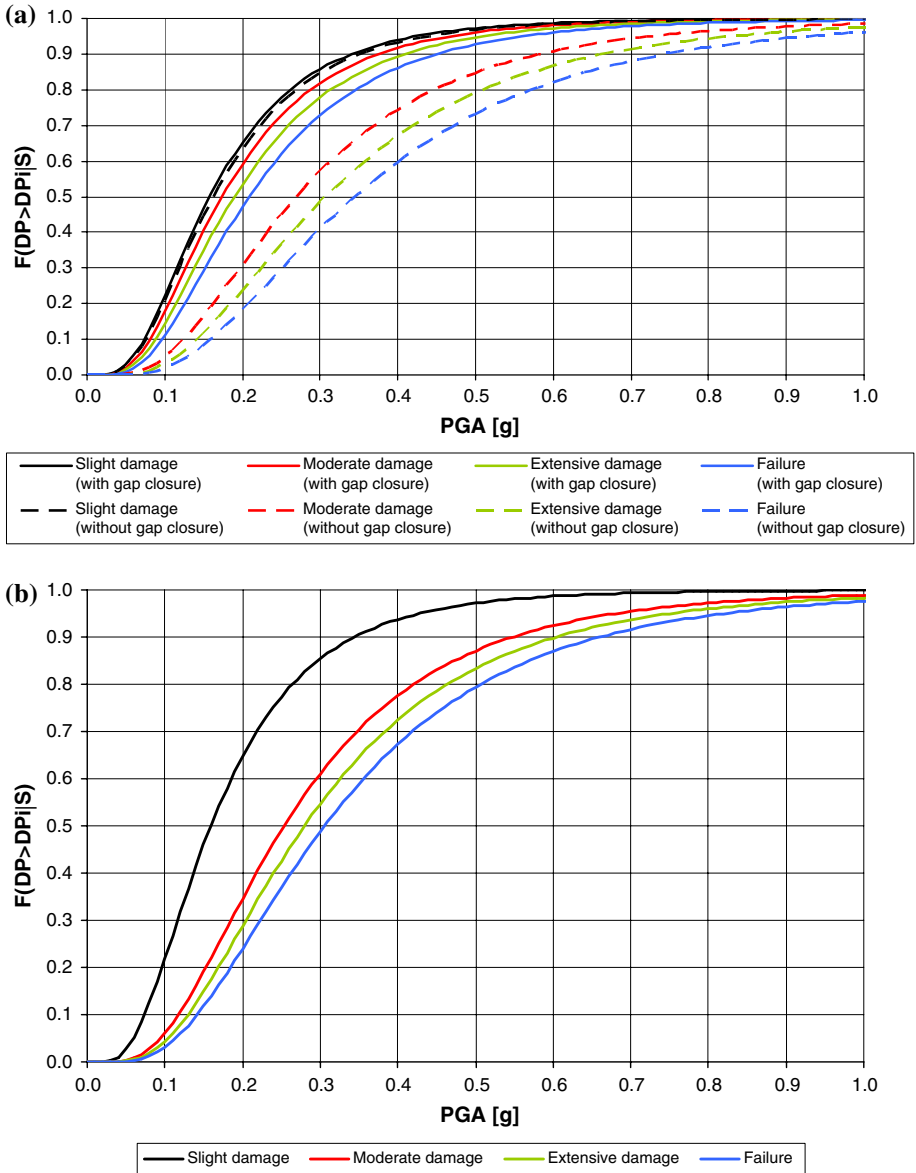


**Fig. 11** Fragility curves of Eirini bridge. (a) Longitudinal direction, (b) Transverse direction

(calculated based on only 40% of the design seismic displacement) closes relatively early (i.e. at a smaller displacement), leading to failure of the bridge in the longitudinal direction, since failure of the abutment-backfill system generally precedes that of the piers.

#### 4.2 Effect of earthquake input

A further important issue is the effect of the earthquake input characteristics on the calculated fragility curves, which several previous studies (e.g. [Karim and Yamazaki 2001](#);

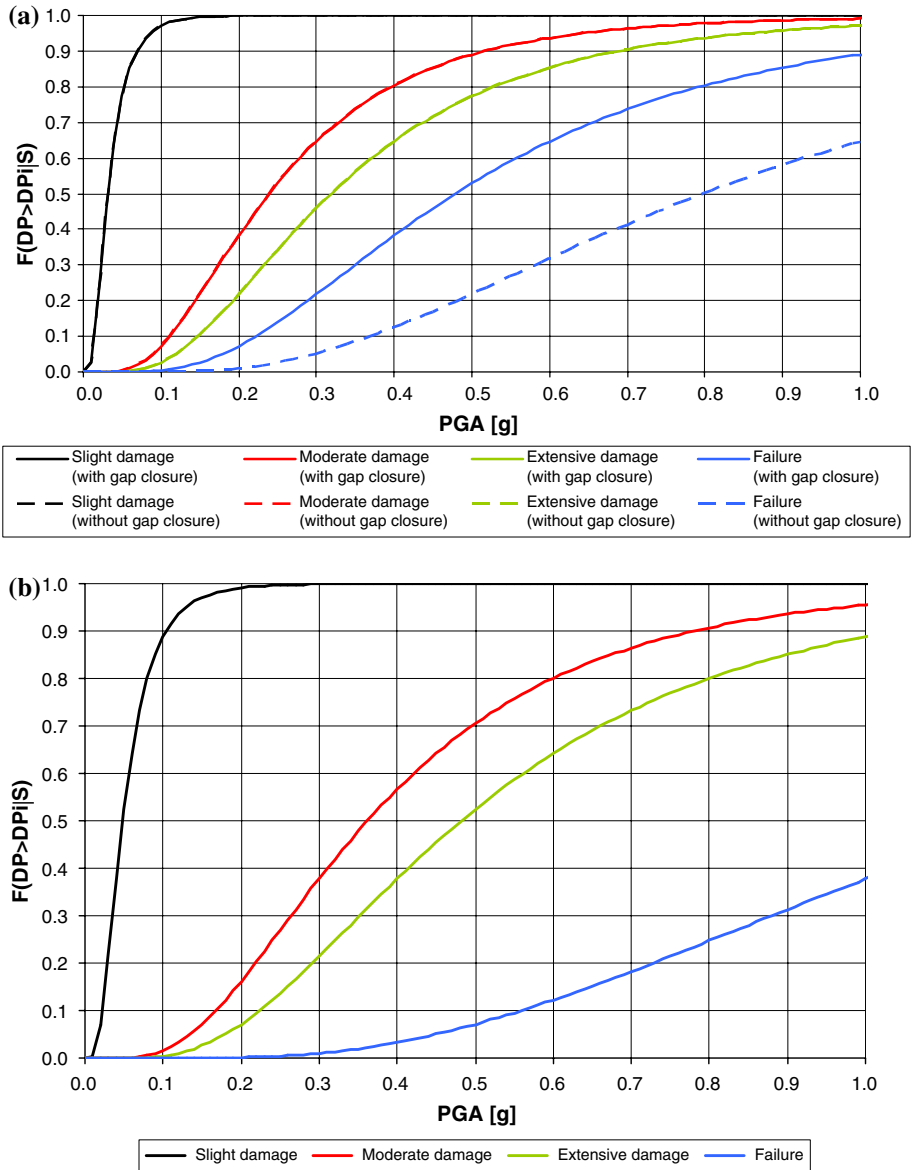


**Fig. 12** Fragility curves of Lissos bridge. **(a)** Longitudinal direction, **(b)** Transverse direction

Choi et al. 2004) have shown to be a major factor. To this effect, apart from the design spectrum of the Greek Code, fragility curves were also derived for the average spectrum of greek earthquakes derived by Athanassiadou et al. (2004) on the basis of a large number (71) of records from greek ground motions. It is noted that in the case of the design spectrum of the Greek Code the spectrum for the soil class pertinent to each bridge was taken into account to derive fragility curves, while in the case of the spectrum from greek earthquakes the average spectrum for all records (corresponding to different site conditions) was used. In Fig. 17a the derived set of fragility curves for bridge G11, in the transverse direction, for the

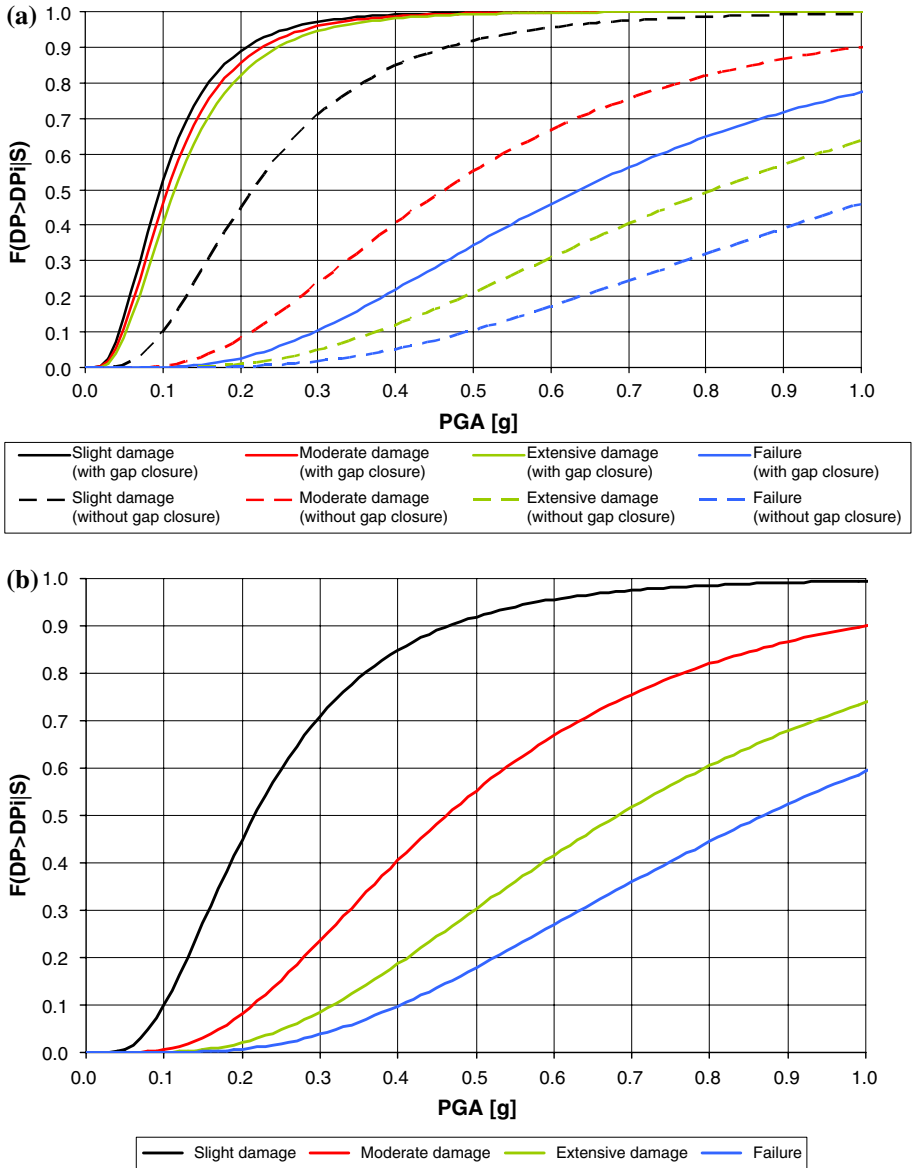


**Fig. 13** Fragility curves of 2nd Kavala Ravine bridge. (a) Longitudinal direction, (b) Transverse direction

mentioned two demand spectra are shown. It is clear that the probability of exceeding a specific damage state for a given seismic intensity reduces significantly if the average spectrum of the greek earthquakes, rather than the design code spectrum, is used in fragility analysis. This can be easily explained if the significant difference between the two spectra for period values longer than about 0.4 s is noted (Fig. 17b), the fundamental period of all the examined bridges being greater than 0.4 s. Moreover, in many bridges (such as bridge G11) the median threshold values of PGA resulted extremely high (greater than 2 g for the damage state DS4-failure/collapse) indicating significant safety margins against failure.

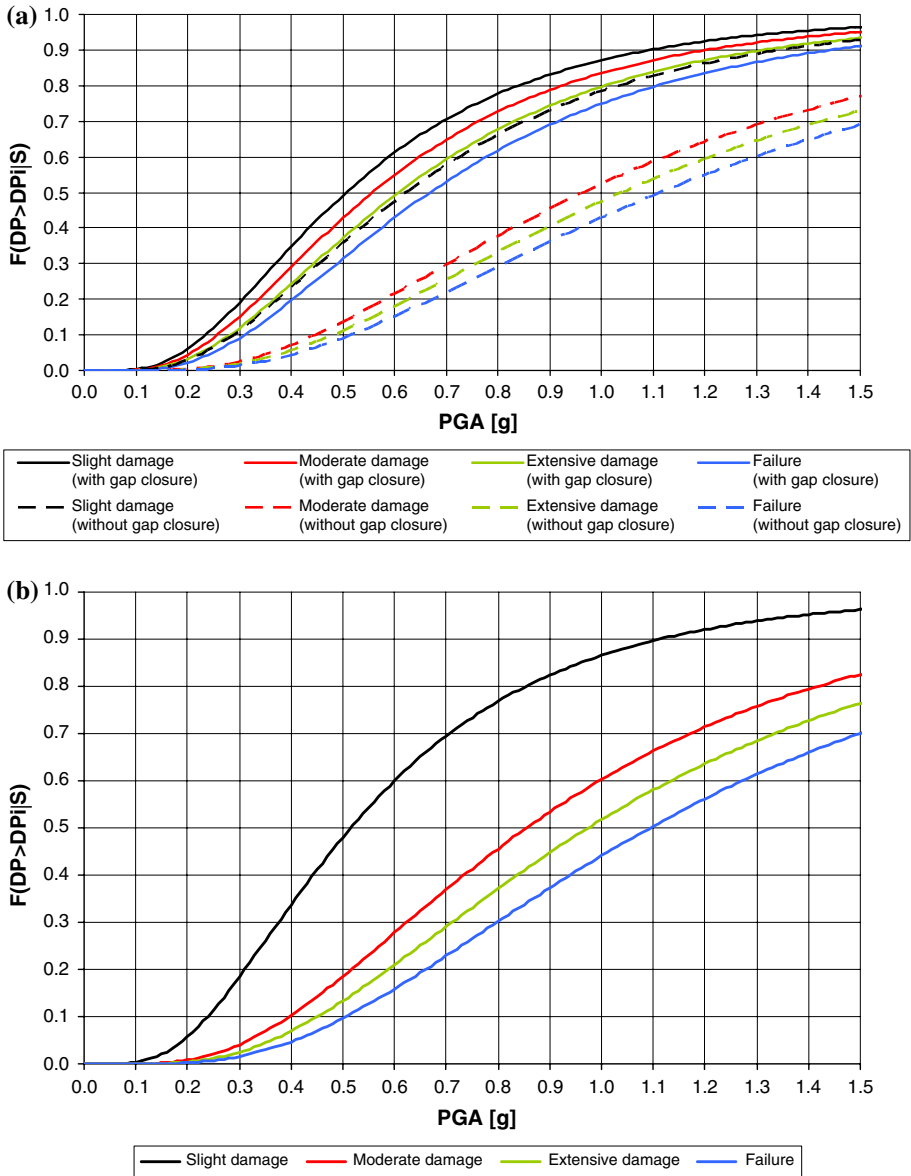


Fig. 14 Fragility curves of G2 bridge. (a) Longitudinal direction, (b) Transverse direction

It is beyond the scope of this paper to discuss the issue of which demand spectra would be more appropriate. Recent work by the ITSAK and University of Thessaloniki groups (Karakostas et al. 2007) has shown that records from intermediate depth earthquakes in Greece give response spectra that are much closer to those of the current Code. In any case, it is clear that in the proposed method (as well as in those based on time-history analysis) the ground motion characteristics have an important effect on the calculated fragility curves.

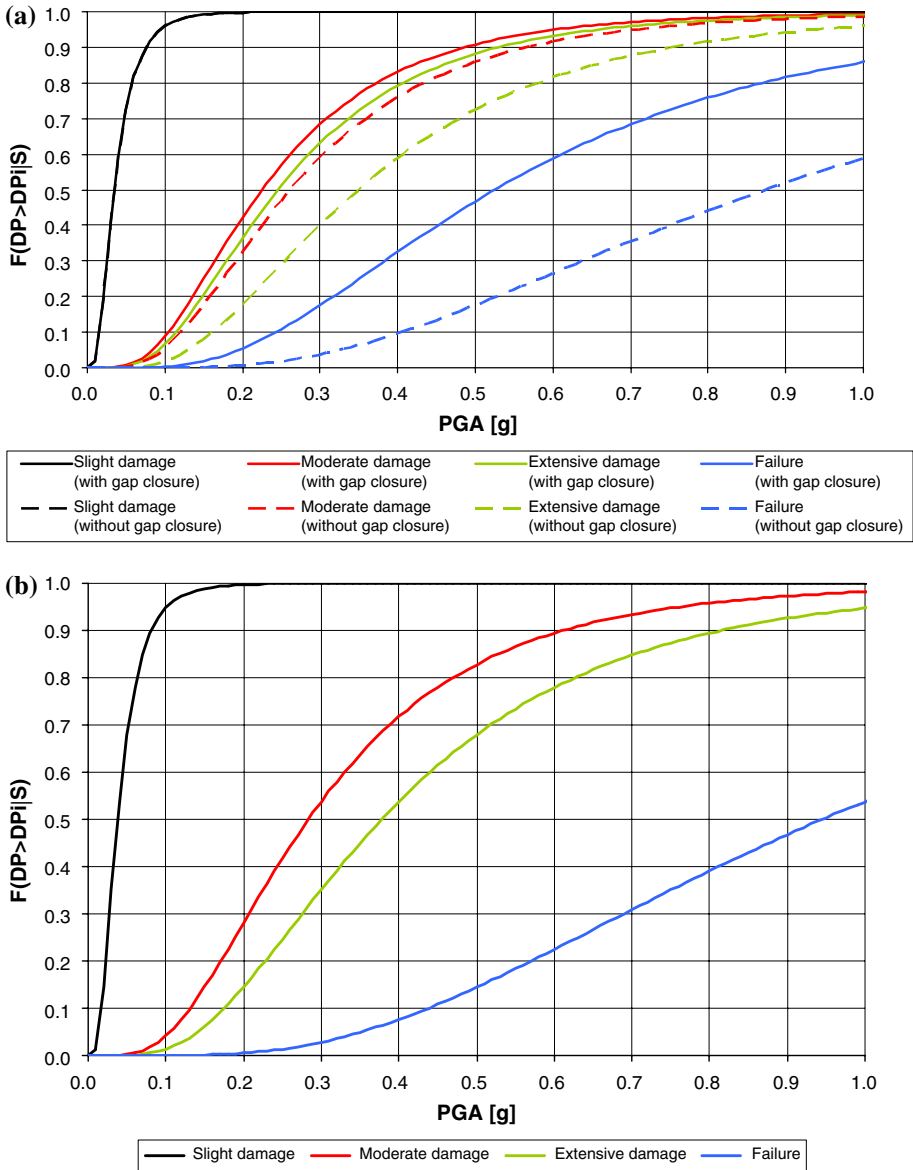
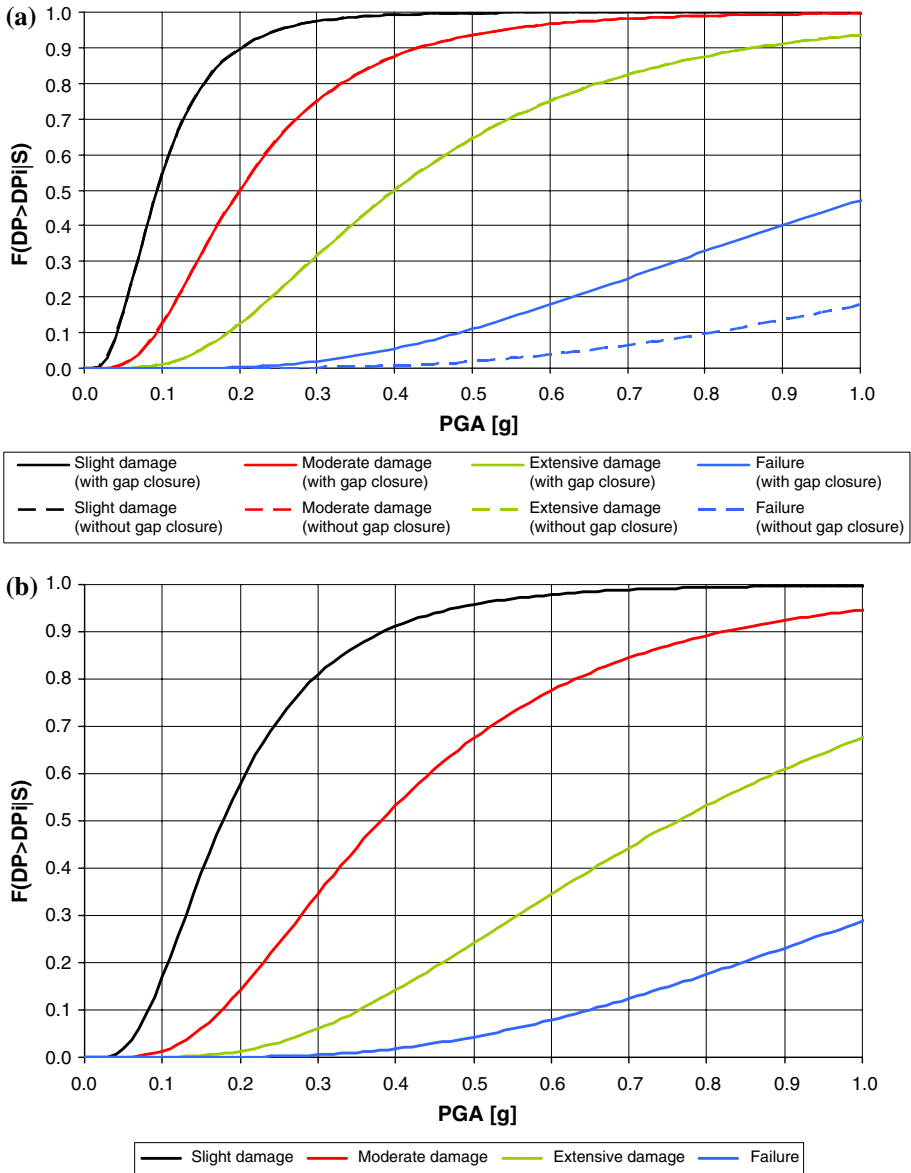


Fig. 15 Fragility curves of Kossynthos bridge. (a) Longitudinal direction, (b) Transverse direction

### 4.3 Effect of analysis procedure

Another critical issue is the sophistication of analysis procedure used for deriving the fragility curves. The curves presented in Figs. 6–16 were derived using pushover analysis, as described in Sect. 3.2. Further sets of capacity curves for some bridge types were derived using dynamic time history analysis. To this purpose five spectrum-compatible accelerograms were generated using the computer code ASING (Sextos et al. 2003). The records were scaled to increasing levels of earthquake intensity, and time-history analysis of the



**Fig. 16** Fragility curves of Krystallopiigi bridge. (a) Longitudinal direction, (b) Transverse direction

bridge model was carried out, to derive a ‘dynamic pushover curve’ i.e. a plot of maximum displacement of the monitoring point versus the base shear that corresponds to the next time step in the analysis (average values for the five records), as discussed in [Paraskeva and Kappos \(2007\)](#).

The bilinear capacity curve derived for bridge T7 (transverse direction) by fitting two lines to the aforementioned points [ $U_{max}(t)$  versus  $V(t+\Delta t)$ ] are shown in [Fig. 18](#), along with the corresponding static pushover curve. It is seen that the dynamic curve is characterised by a slightly higher strength and is slightly “stiffer” than the corresponding standard



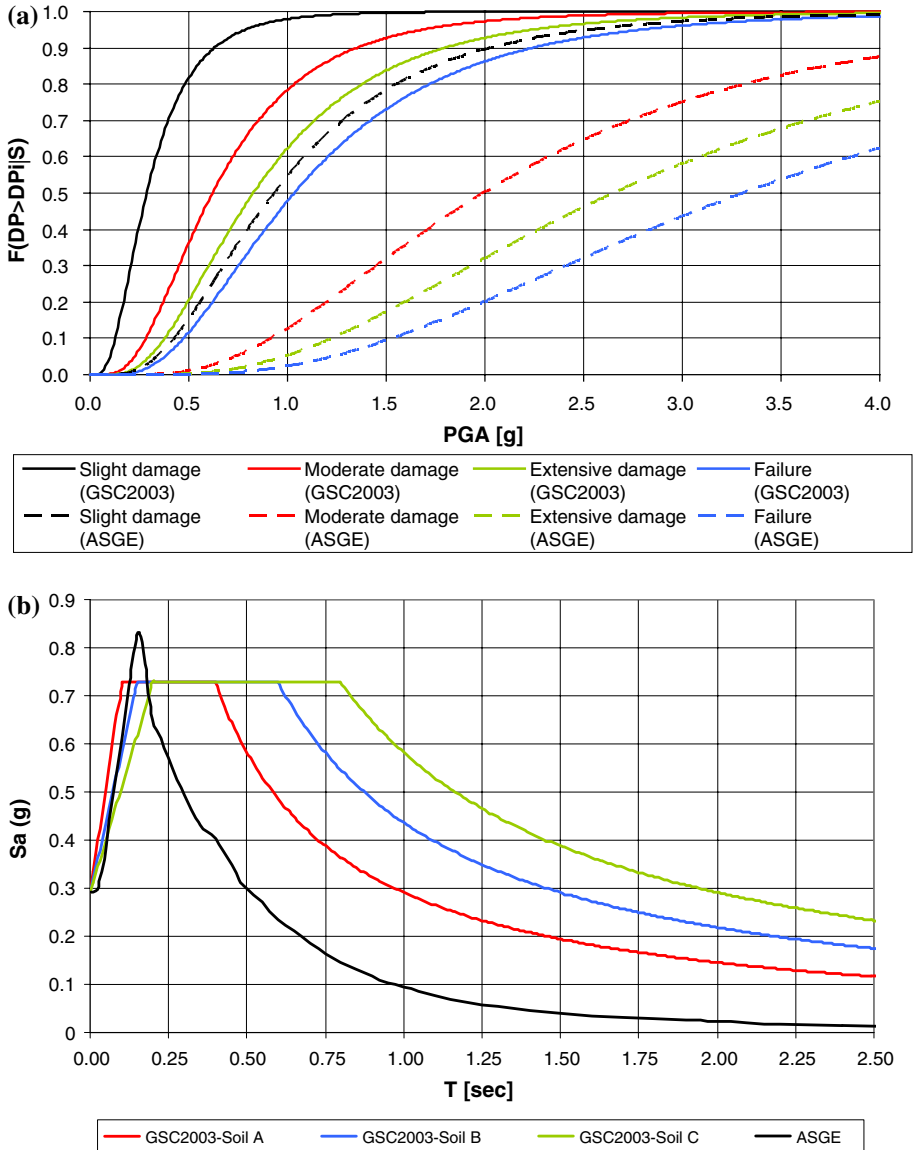


**Fig. 17** Effect of demand spectrum on fragility curves. **(a)** Fragility curves of G11 bridge in the transverse direction, **(b)** Comparison between average spectrum of greek earthquakes (ASGE) and design spectra of Greek Code (GRSC2003)

pushover curve in both the elastic and the post-elastic branch. As a consequence, fragility curves derived using the dynamic pushover curves lie on the left of the corresponding curves derived using the static pushover curves (Fig. 19). It is clear that so long as the basic assumptions, such as the dynamic input (spectrum), the definition of damage states, etc. are the same, differences in the fragility curves resulting from the type of analysis used are minor.

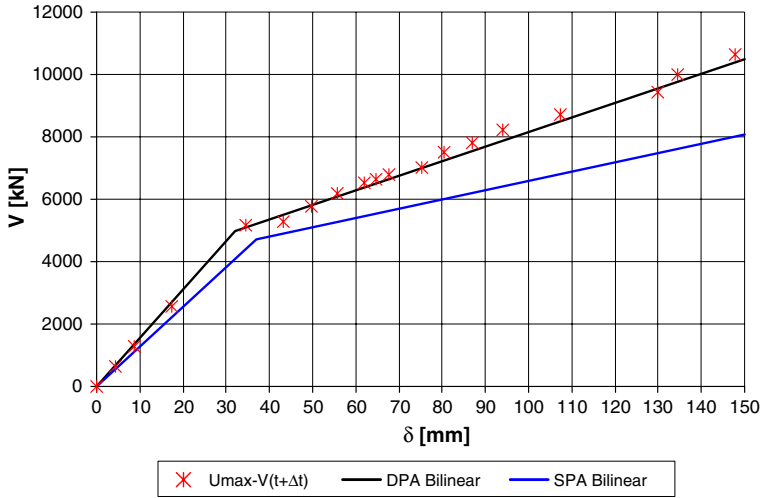


Fig. 18 Pushover curves for T7 bridge for different analysis methods

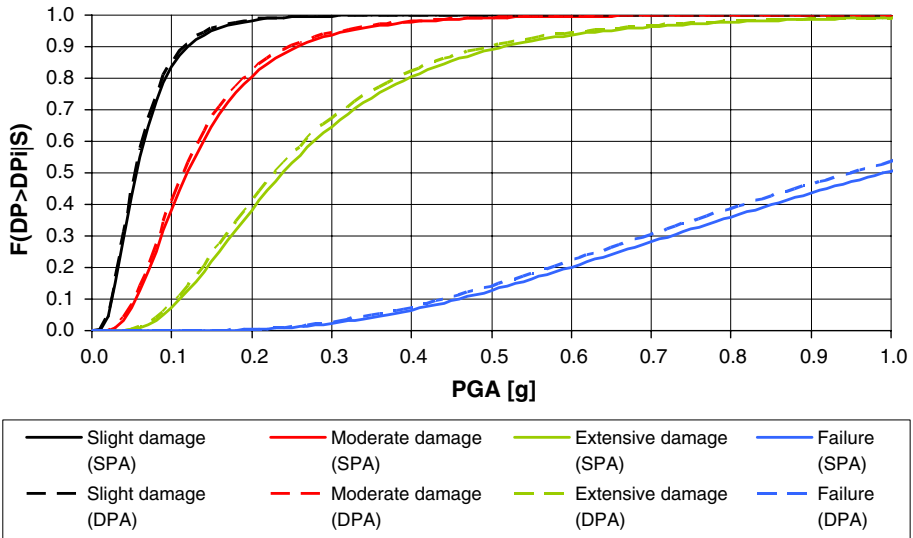
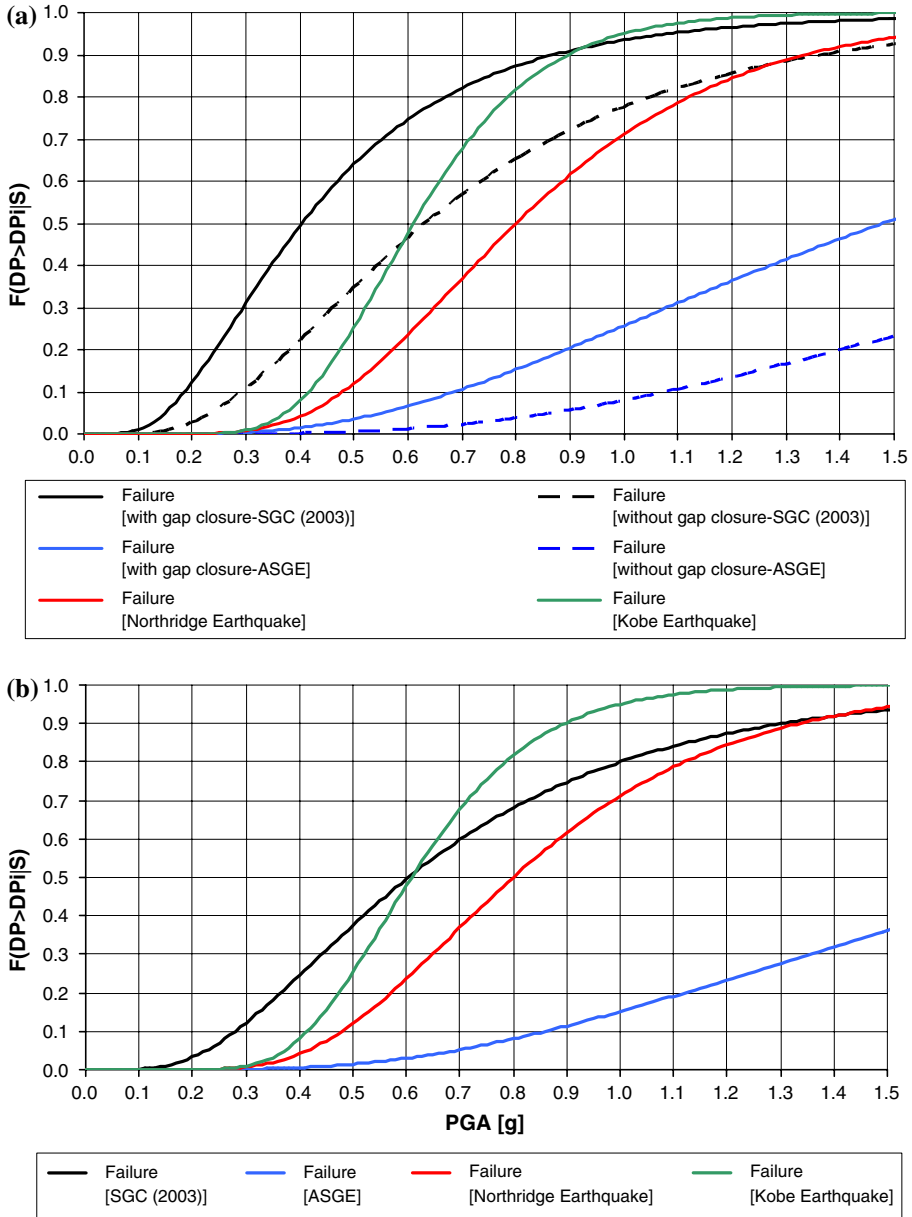


Fig. 19 Fragility curves for T7 bridge using pushover and time-history analysis

4.4 Calibration against empirical data

A first attempt was made to calibrate the derived fragility curves on the basis of actual bridge damage data from the US and Japan, given the absence of such data from greek or other european earthquakes. Such an attempt is, obviously, subject to several limitations, nevertheless it can provide some qualitative information relevant to various parameters that may affect a bridge’s seismic response, which are very difficult to include in the framework of an analytical methodology. As an example, in Fig. 20, the analytically



**Fig. 20** Comparison of analytically derived fragility curves for Pedini bridge with empirical fragility curves from Japan and the US. (a) Longitudinal direction, (b) Transverse direction

derived fragility curves for Pedini bridge, for damage state DS4 (Failure/Collapse) are plotted against the empirical fragility curves derived on the basis of observed damage data from Northridge (Basöz et al. 1999) and Kobe (see EQE 2000) earthquakes. It should be emphasised here that empirical fragility curves are available for no more than three damage states.

Assuming that the analytically derived fragility curves based on the Greek code spectrum are the lower limit and the corresponding ones for the average spectrum of the 71 greek earthquakes are the upper limit, it would be expected that the empirical fragility curves for the seismic events in the USA and Japan lied between the two aforementioned limits. Indeed, this was observed for all damage states in the longitudinal direction of the 11 bridges examined (an example is shown in Fig. 20), especially in the case where the abutment-backfill effect is taken into account, even when the approximate threshold values are used. On the contrary, in the transverse direction of the examined bridges in many cases the empirical fragility curves lied either on the right of the upper limit (smaller probability of exceeding a specific damage state for a given earthquake intensity) or on the left of the lower limit (greater probability of exceeding a specific damage state for a given earthquake intensity). The former case, i.e. being on the 'safe' side, might be due to, on the one hand, the underestimation of several aspects of bridge capacity (strength, ductility, yielding and failure of bearings), and on the other hand by the effect of various phenomena not taken into account during the modelling of the bridge (such as soil–structure interaction, ignored in most cases). Inversely, the latter case, i.e. being on the 'unsafe' side, could be related to the overestimation of various bridge characteristics mentioned before. It should be pointed out here that the empirical fragility curves refer to concrete bridges in general, since data for specific categories were generally found (Basöz et al. 1999) to be insufficient for calibration purposes.

## 5 Conclusions

The main objective of this study was to assess the seismic vulnerability of bridges in Greece. A classification system was first developed and then a new analytical methodology for deriving bridge fragility curves was proposed, wherein damage state definition differs according to the bridge energy dissipation mechanism, i.e. bridges with yielding piers of the column type and bridges with bearings and non-yielding piers of the wall type. Another key aspect taken into account was the effect of the abutment-backfill system due to the gap closure between the deck and the abutments of the bridge; hence all potentially critical components of the bridge are considered in the development of fragility curves. The proposed procedure was applied to three-dimensional models of 11 'generic' bridges, one from each class defined in the classification scheme, which are deemed to fairly represent the most common typologies found in modern motorways in Greece and several other European countries.

Similarities but also important differences were noted in the derived fragility curves, which indicates that it is not easy to group them into one or two 'general' fragility curves, as done in some previous studies. Comparisons of the fragility curves developed for each direction of the bridges show that the critical direction is the longitudinal one if the definition of the critical direction is based on the higher two damage states (DS3 and DS4); however this is not generally the case for the lower two damage states, particularly for bridges with bearings, wherein damage in the longitudinal direction of bearings is uniform, whereas in the transverse direction the shear deformation of the bearings reduces towards the abutments (the exception being the case where transverse displacement at the abutments is not restrained). Another important finding was that the derived fragility curves were heavily dependent on the spectra used for estimating demands (two different types of spectra were used, that of the Greek Seismic Code and that resulting from the study by Athanassiadou et al.).

Finally, the analytically derived fragility curves were subjected to a first, qualitative, calibration against empirical curves based on damage data from the US and Japan, due to the absence of corresponding data from european earthquakes. This comparison has shown that

the empirical fragility curves generally lie between the two limits defined by the different sets of analytically derived fragility curves (corresponding to the different type of spectra used) for the longitudinal direction of the 11 bridge classes; however, no clear trends were found in the curves for the transverse direction. In any case it is clear that more work is needed towards calibration of the fragility curves derived for European bridges; this remark also holds for most of the fragility curves developed world-wide, and the main reason is the absence of sufficient seismic damage data for bridges, in contrast to the case of buildings.

**Acknowledgements** As mentioned in the Introduction, a number of research teams from both the academic and research community, and from engineering design offices, have participated in the ASProGe Project, funded by the General Secretariat of Research and Technology of Greece. In addition to the authors of this paper, significant contributions to the research reported herein were made by Ms. Th. Paraskeva and Dr. A. Sextos (University of Thessaloniki), Prof. M. Papadrakakis and Mr. C. Papanikolopoulos (NTU, Athens), Dr. C. Karakostas and Dr. V. Lekidis (ITSAK, Thessaloniki), Dr. D. Konstantinidis (Egnatia Odos SA), and Dr. K. Stathopoulos, Dr. S. Vlachos, and Dr. S. Stathopoulos (DOMI SA).

## References

- Applied Technology Council [ATC] (1985) Earthquake damage evaluation data for California. Report ATC-13, Applied Technology Council, Redwood City, CA
- ATC (1996) Seismic evaluation and retrofit of concrete buildings. Rep. No. SSC 96-01: ATC-40, 1, Redwood City, CA
- Athanassiadou C, Karakostas C, Kappos AJ, Lekidis V (2004) Inelastic strength and displacement design spectra based on Greek earthquake records. In: 13th world conference on earthquake engineering. Vancouver, CD ROM Proceedings, Paper no. 2519
- Basöz NI, Kiremidjian AS, King SA, Law KH (1999) Statistical analysis of bridge damage data from the 1994 Northridge, CA, earthquake. *Earthquake Spectra* 15(1):25–54
- Cardone D, Perrone G, Dolce M (2007) Seismic risk assessment of highway bridges. In: Proceedings 1st US–Italy seismic bridge workshop. IUSS Press Ltd, Pavia (Italy)
- Choi E, DesRoches R, Nielson B (2004) Seismic fragility of typical bridges in moderate seismic zones. *Eng Struct* 26(2):187–199
- Computers and Structures Inc (2005) SAP2000: linear and non linear static and dynamic analysis and design of three-dimensional structures. Berkeley, California
- Dutta A, Mander JB (1998) Seismic fragility analysis of highway bridges, INCEDE-MCEER center-to-center. In: Proceedings of the center-to-center workshop on earthquake engineering frontiers in transport systems, Tokyo, Japan, pp 311–325
- EQE International (2000) Seismic risk assessment tool: specification document. Prepared for Egnatia Odos A.E. Report no. 460-01-RS-01, Issue 1
- Erduran E, Yakut A (2004) Drift based damage functions for reinforced concrete columns. *Comput Struct* 82(2–3):121–130
- Fajfar P (1999) Capacity spectrum method based on inelastic demand spectra. *Earthquake Eng Struct Dyn* 28(9):979–993
- FEMA-NIBS (2004) Multi-hazard loss estimation methodology—earthquake model: HAZUS@MH Technical Manual, Washington, DC
- FHWA [Federal Highway Administration] (1995) Recording and coding guide for the structure inventory and appraisal of the nation's bridges. Rep. no. FHWA-PD-96-001, Office of Engineering, Bridge Division, Washington, DC
- Gardoni P, Khalid MM, Kiureghian AD (2003) Probabilistic seismic demand models and fragility estimates for RC bridges. *J Earthquake Eng* 7(1):79–106
- Hwang H, Jernigan JB, Lin YW (2000) Evaluation of seismic damage to Memphis bridges and highway systems. *J Bridge Eng ASCE* 5(4):322–330
- Kappos AJ, Moschonas IF, Paraskeva T, Sextos AG (2006) A methodology for derivation of fragility curves for bridges with the aid of advanced analysis tools. In: 1st European conference on earthquake engineering and seismology, Geneva, Switzerland, Paper no. 275
- Kappos AJ, Potikas P, Sextos AG (2007) Seismic assessment of an overpass bridge accounting for non-linear material and soil response and varying boundary conditions. In: Proceedings of the conference on

- computational methods in structural dynamics and earthquake engineering (COMPdyn), Rethymno, Greece, Paper no. 1580
- Karakostas CZ, Athanassiadou CJ, Kappos AJ, Lekidis VA (2007) Site-dependent design spectra and strength modification factors, based on records from Greece. *Soil Dyn Earthquake Eng* 27(11):1012–1027
- Karim KR, Yamazaki F (2001) Effect of earthquake ground motions on fragility curves of highway bridge piers based on numerical simulation. *Earthquake Eng Struct Dyn* 30(12):1839–1856
- Lupoi A, Franchin P, Pinto PE, Monti G (2005) Seismic design of bridges accounting for spatial variability of ground motion. *Earthquake Eng Struct Dyn* 34(4–5):327–348
- Mackie KR, Stojadinovic B (2007) R-factor parameterized bridge damage fragility curves. *J Bridg Eng ASCE* 12(4):500–510
- Mander JB, Basöz N (1999) Seismic fragility curve theory for highway bridges. In: Proceedings of the 5th US conference on lifeline earthquake engineering, TCLEE No. 16, ASCE, 1999, pp 31–40
- Monti G, Nistico N (2002) Simple probability-based assessment of bridges under scenario earthquakes. *J Bridg Eng ASCE* 7(2):104–114
- Paraskeva T, Kappos A (2007) Seismic assessment of an over-cross bridge using modal pushover analysis and dynamic time-history analysis. In: Proceedings of the conference on computational methods in structural dynamics and earthquake engineering (COMPdyn), Rethymno, Greece, Paper no. 1376
- Paraskeva T, Kappos A, Sextos A (2006) Extension of modal pushover analysis to seismic assessment of bridges. *Earthquake Eng Struct Dyn* 35(10):1269–1293
- SETRA [Service d' Etudes Techniques des Routes et Autoroutes] (1998) Typologie IQOA—Valise de formation IQOA Ponts. Ministère de l' Equipement, des Transports, etc, France
- Sextos A, Ptilakis K, Kappos A (2003) Inelastic dynamic analysis of RC bridges accounting for spatial variability of ground motion, site effects and soil–structure interaction phenomena. Part 1: methodology and analytical tools. *Earthquake Eng Struct Dyn* 32(4):602–627
- Shinozuka M, Feng MQ, Kim HK, Kim SH (2000) Nonlinear static procedure for fragility curve development. *J Eng Mech ASCE* 126(12):1287–1295